ACS OMEGA

Open Access

http://pubs.acs.org/journal/acsodf

Article

Serum *N*-Glycan Profiling of Patients with Narcolepsy Type 1 Using LC-MS/MS

Akeem Sanni,◆ Md Abdul Hakim,◆ Mona Goli, Moyinoluwa Adeniyi, Farid Talih, Bartolo Lanuzza, Firas Kobeissy, Giuseppe Plazzi, Monica Moresco, Stefania Mondello, Raffaele Ferri, and Yehia Mechref*

Cite This: *ACS Omega* 2024, 9, 32628−32638

Read Online

ACCESS | Metrics & More | Article Recommendations | Supporting Information

ABSTRACT: The neurological condition known as narcolepsy type 1 (NT1) is an uncommon condition marked by extreme daytime sleepiness, cataplexy, sleep paralysis, hallucinations, disrupted nocturnal sleep, and low or undetectable levels of orexin in the CSF fluid. NT1 has been hypothesized to be an immunological disorder; its treatment is currently only symptomatic, and misdiagnosis is not uncommon. This study compares the *N*-glycome of NT1 patients with healthy controls in search of potential glycan biomarkers using LC-MS/MS. A total of 121 candidate *N*-glycans were identified, 55 of which were isomeric *N*-glycan structures and 65 were not. Seventeen *N*-glycan biomarker candidates showed significant differences between the NT1 and control cohorts. All of the candidate glycan biomarkers were isomeric except $HexNAc_6Hex_7Fuc_0NeuAc_1$ (6701) and $HexNAc_6Hex_7Fuc_1NeuAc_2$ (6712). Therefore, with isomeric and nonisomeric structures, a total of 20 candidate *N*-glycan biomarkers are reported in this study, and interestingly, all are either sialylated or sialylated-fucosylated and upregulated in NT1 relative to the control. The distribution levels of all the identified *N*-glycans show that the sialylated glycan type is the most abundant in NT1 and is majorly disialylated, although the trisialylated subtype is three-fold higher in NT1 compared to the healthy control. The first isomers of $HexNAc_5Hex_6Fuc_0NeuAc_3$ (5603), $HexNAc_6Hex_7Fuc_0NeuAc_2$ (6702), and $HexNAc_6Hex_7Fuc_1NeuAc_4$ (6714) expressed a high level of fold changes (FC) of 1.62, 2.19, and 2.98, respectively. These results suggest a different *N*-glycome profile of NT1 and a relationship between sialylated glycan isomers in NT1 disease development or progression. The revelation of *N*-glycan expression alterations in this study may improve NT1 diagnostic methods, understanding of NT1 pathology, and the development of new targeted therapeutics.

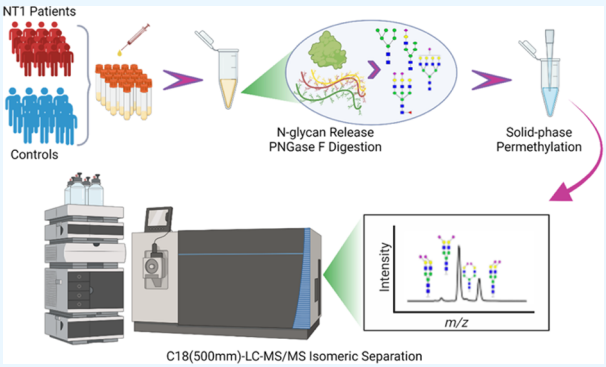

INTRODUCTION

Narcolepsy type 1 (NT1), commonly known as narcolepsy with cataplexy, is a neurological condition characterized by excessive daytime sleepiness, cataplexy, sleep paralysis, hallucinations, disturbed nocturnal sleep, and low detection or undetectable levels of orexin in the biofluids. Previously, NT1 has been hypothesized to be an immunological illness; however, its treatment is currently only symptomatic, and misdiagnosis is not uncommon.[1] NT1 is distinguished by the selective loss of hypocretin-orexin neurons in the hypothalamus, leading to a reduction in the levels of the hypocretin-1/orexin A neurotransmitter.[2] The main cause of hypocretin/orexin neuron loss is complex and not fully known, but studies suggest genetic, environmental, and autoimmune factors.[3,4] The orexinergic system dysfunction can also influence other metabolic processes, including type 2 diabetes and obesity, thereby complicating disease diagnosis and prognosis of NT1.

Previously, alterations in the serum proteome of the NT1 patient have been evaluated in search of candidate biomarkers; however, to the best of our knowledge, the serum glycome has not been profiled.[5] Protein glycosylation is a complex and heterogeneous post-translational process of carbohydrates' attachment to proteins. These complex sugars are highly involved in vital biological processes such as maintaining the structural integrity of proteins, assisting in their proper folding, and facilitating communication and adhesion between cells.[6,7] Glycomics differs from glycoproteomics analysis in that glycomics is constrained to the exclusive analysis of glycans, while the latter provides valuable insights into the presence of glycoforms and their occupancy on protein sites.[8] Nevertheless, through the adept utilization of a diverse array of derivatization and separation techniques, glycomics achieve higher sensitivity and enhanced separation efficiency. Consequently, this

Received: February 19, 2024
Revised: May 17, 2024
Accepted: May 27, 2024
Published: July 16, 2024

https://doi.org/10.1021/acsomega.4c01593
ACS Omega 2024, 9, 32628−32638

approach enables the thorough characterization of minor glycan structures and isomers, thus significantly enhancing our understanding of glycan complexity and diversity.[8] Glycans have been reported to act as receptors during influenza pathogenesis, further pointing to their role in the host−pathogen relationship.[9] Anomalous glycosylation has been suggested as a biomarker for a number of disorders, including Alzheimer's disease (AD) and Parkinson's disease (PD). Changes in the glycosylation of proteins have also been connected to breast cancer, ovarian cancer, and neurological diseases, and due to glycan microheterogeneity, they can exhibit many isomers.[10−16] These glycan isomers further increase the glycan complexity. Studies have identified the relevance of glycan isomers in several diseases, and it has been explored in biomarker studies and early disease diagnosis.[17,18] Despite the biological relevance of *N*-glycan isomers, their identification and quantification have been a challenge. Several methods have been employed to improve their specific identification and quantification, but these methods are not without limitations.[19] Nuclear Magnetic resonance (NMR) does have the ability to give *N*-glycan stereochemistry and primary structure but requires a large, pure sample size for analysis.[20] Mass spectrometry (MS) is commonly used to unravel the complex structures of glycans and glycoproteins. It has become an enormously powerful tool to analyze complex biological samples, which helps understand the activities of modified proteins in biological systems and the underlying causes of associated disease progression.

However, MS alone cannot efficiently separate the isomers of glycans and glycopeptides. That is why high-performance liquid chromatography (HPLC) hyphenated with MS has been utilized to perform better separation of isomeric structures, followed by the identification and quantification of those structures. Liquid chromatography combined with mass spectrometry (LC-MS) has been shown to be a highly effective technology for the qualitative and quantitative investigation of glycans and their isomers due to its great sensitivity and selectivity.[19,21,22]

Advancements in MS-based techniques have revolutionized the analysis of glycans in biological samples, fostering a deeper understanding of their roles in various biological processes. Among these techniques, *N*-glycan permethylation stands out as a pivotal method offering several benefits over native glycans.[23] Permethylation substantially increases the hydrophobicity through the replacement of the active hydrogens from hydroxyl and amine groups of the glycans with methyl groups. It improves the ionization efficiency, prevents fucose migration and sialic acid loss during the MS analysis, and, thereby, enhances the sensitivity and fragmentation of glycans in MS analysis.[24,25] This capability is invaluable for distinguishing between glycan isomers and unraveling intricate glycan structures critical for understanding their functional roles.[26]

There are different separation techniques and columns that are commonly used to separate glycan and their isomers such as the C18 column and hydrophilic interaction chromatography (HILIC) column. The HILIC columns can be used to efficiently separate native glycans and their isomers, which are more hydrophilic in nature;[22,,28] however, due to the high hydrophobicity, permethylated glycans and their isomers are better separated in reverse-phase chromatography using the C18 column.[19,29,30] The interaction between the hydrophobic tags on permethylated glycans and the stationary phase of the C18 column enhances the separation efficiency.[31] This enables precise isomeric separation, allowing researchers to discriminate between structurally similar glycans with unparalleled accuracy.[29,32]

MS/MS offers the advantage of precursor ion fragmentation using different dissociation techniques such as collision-induced dissociation (CID), higher-energy collision dissociation (HCD), electron-transfer/higher-energy collision dissociation (EThcD), and many others.[33,34] These fragmentation techniques retain the structural information on the product ion, thereby improving the accuracy of biomolecular structural elucidation with high sensitivity and selectivity and also improving the confidence of quantitation. With these methods, extensive structural information for high-throughput identification of biomolecules like glycans in a complex sample can be achieved.[21,35−39] Biomarker research has been revolutionized by MS/MS, which can detect, recognize, and characterize molecules as indicators of diseases. The advancements in MS/MS technology have made it more efficient in identifying candidate biomarkers and detecting biomolecules. In addition, MS/MS has the potential to offer significant insights into disease states and therapeutic targets, and its importance is expected to increase as the technology advances.[40,41]

In this research, the primary objective was to profile the serum *N*-glycome of NT1, find their correlation with the progression of the disease, and compare that to the previously reported potential biomarkers of other neurodegenerative diseases such as Alzheimer's diseases, Parkinson's disease, restless leg syndrome (RLS), etc. In order to meet this goal, the LC-MS/MS approach was utilized to successfully identify differentially expressed serum *N*-glycans, which might be considered potential biomarkers for NT1 after further studies.

METHODS

Clinical Information of Patients Included in the Study.

Patients with NT1 clinical diagnoses were recruited between April and June 2018 at the Sleep Research Center from the Oasi Research Institute-IRCCS, Troina, and the Sleep Disorders Center, Center for Narcolepsy, IRCCS Institute of Neurological Sciences, Bologna in Italy. The third edition of the International Classification of Sleep Disorders requires a clinical and laboratory diagnosis of NT1 for people with the condition and that the following criteria are met: unambiguous cataplexy, persistent daytime sleepiness, at least two sleep-onset rapid eye movement (REM) periods at the multiple sleep latency test (including the eventual sleep-onset REM period recorded during the receding night polysomnography, mean sleep latency <8 min), and, when available, evidence of orexin A deficiency in the cerebrospinal fluid.[42] All patients had the human leukocyte antigen (HLA) DQB1*0602 haplotype assessed. HLA DQB1*0602 is a type of HLA class II molecule, which is known for presenting antigenic peptides to CD4+ T cells, thereby playing a principal role in the immune system; and previous studies have reported a strong association between HLA and narcolepsy.[3,43−45] Patients with any other neurologic or medical issues, such as diabetes or hypertension, or those on any drugs were excluded from the study. All patients were recruited quickly after the diagnosis; thus, all were drug-naive at the time of blood sample collection. None of these individuals had H1N1 influenza or Streptococcus infection or received AS03-adjuvanted vaccination before developing narcoleptic symptoms. Controls were participants without NT1. The regional ethics committee approved the study, and each subject submitted written informed consent before participating.

https://doi.org/10.1021/acsomega.4c01593
ACS Omega 2024, 9, 32628−32638

Demographic data and some clinical details are reported for each participant, and the summary is presented in Table 1.

Table 1. Biological Information on Human Study Participants

general information	NT1	control
number of subjects	11	11
gender (male/female)	7/4	7/4
age (years)	19−71	28−73
presence of HLA DQB1*0602 allele	10	2
cerebrospinal fluid orexin level (pg/mL)	0−119.6	not available

Materials and Reagents. Ammonium bicarbonate (ABC), dimethyl sulfoxide (DMSO), sodium hydroxide beads, and iodomethane were obtained from Sigma-Aldrich (St. Louis, MO). HPLC-grade water, acetonitrile (ACN), methanol, and mass spectrometry grade formic acid (FA) were purchased from Fisher Scientific (Fair Lawn, NJ). Peptide-*N*-glycosidase F (PNGase F) was acquired from New England Biolabs (Ipswich, MA). Empty spin columns were purchased from Harvard Apparatus (Holliston, MA).

Sample Preparation for *N*-Glycan Profiling in NT1 and Healthy Serum Samples. A 10 μL aliquot of human serum was transferred to an Eppendorf tube and diluted 10 times with the ABC buffer. The glycoproteins were denatured at 90 °C for 15 min. The samples were cooled to room temperature, and then 1 μL of PNGase F enzyme was added and incubated for 18 h to release the glycans from the peptide backbone. Enough ethanol was added to the samples to make a final concentration of 90% ethanol, and samples were placed at −20 °C for 1 h to precipitate the proteins. The samples were centrifuged at 14,800 rpm for 10 min, and then the supernatant was collected and dried in a SpeedVac evaporator.

Ten microliter aliquot of the borane ammonia complex (10 μg/μL) was added to each sample before being incubated for an hour at 60 °C to reduce the end of the glycans. One thousand microliters of methanol was added to the samples, followed by drying in SpeedVac to remove excess borane ammonia. The methanol wash was repeated four more times until the white residue of the borane ammonia completely disappeared. Solid-phase permethylation was performed using iodomethane.[25,46] The dried samples were resuspended in 30 μL of dimethyl sulfoxide (DMSO) and 1.2 μL of water. The empty spin columns were filled with NaOH beads stored in DMSO. The spin columns were centrifuged at 1800 rpm for 2 min, and then the columns were washed again with an additional 200 μL of DMSO. Twenty microliters of iodomethane was added to the sample, mixed, and then loaded to the spin column. The samples were then incubated in the dark at room temperature for 25 min. An additional 20 μL of iodomethane was added to the samples in the spin column and incubated for 15 min. The samples were centrifuged at 1800 rpm for 2 min, followed by the addition of 30 μL of acetonitrile and further centrifugation. The permethylated samples were dried and resuspended in 80% water, 20% ACN containing 0.1% formic acid, and analyzed in LC-MS/MS

LC-MS/MS Conditions for *N*-Glycan Profiling in NT1 and Healthy Serum Samples. All permethylated glycan samples were analyzed in a Dionex 3000 UltiMate Nano LC system (Thermo Scientific, Sunnyvale, CA) coupled to an Orbitrap Fusion Lumos Tribrid Mass Spectrometer (Thermo Scientific, San Jose, CA). The samples were cleaned and purified using a C18 Acclaim PepMap trap column (75 μm × 20 mm, 3 μm, 100 Å; Thermo Scientific, Sunnyvale, CA). The glycans and glycan isomers were separated in a C18 Acclaim PepMap RSLC column (75 μm × 500 mm, 2 μm, 100 Å, Thermo Scientific, Sunnyvale, CA) at 60 °C with a 200 min gradient and a 0.2 μL/min flow rate. The mobile phase A was 98% H_2O and 2% ACN containing 0.1% FA; the mobile phase B was 100% containing 0.1% FA. At the beginning of the run, 20% mobile phase B was maintained for 33 min, followed by increasing quickly to 42% mobile phase B over 4 min. The mobile phase B was further increased to 55% for the next 123 min and then to 90% in 3 min and kept constant for 17 min. Then, the mobile phase B was decreased to the initial condition (20%) in 3 min and remained unchanged until the end of the run. The full MS spectra were acquired with a scan range of 400−2000 m/z at a resolution of 120,000 and a mass accuracy of 10 ppm. The top 20 most intense ions were subjected to MS^2 using CID at 30% normalized collision energy, 60,000 orbitrap resolution, 10 ms activation time, and 0.25 activation Q.

Data Processing and Statistical Analysis of *N*-Glycans in NT1 and Healthy Serum Samples. All *N*-glycans were manually identified prior to the peak integration using Thermo FreeStyle 1.4 SP2 software, and their MS/MS spectra were verified. This gave the ability to authenticate a true peak before quantitation. This was achieved by comparing the experimental m/z values of monoisotopic peaks of glycans in the MS spectra to those obtained with the software within a mass accuracy of 10 ppm. The area under the peaks in the extracted ion chromatograms (EICs) was integrated, and the data generated were transformed into relative abundances of the identified *N*-glycans and isomers in both NT1 (Table S1) and control cohorts (Table S2). The peak areas of all of the glycans and their isomers were summed for individual samples, and then the peak areas of each glycan and each isomer were divided by the sum of the peak areas of all glycans including their isomers to find the relative abundance of each glycan and isomer. The relative abundance percentage and standard deviation across the biological replicates of NT1 and control cohorts are given in Table S3. Every charge state and adduct that might be present in a glycan composition was accounted for. Therefore, the quantitation data were the sum of matching charge states and adducts of a specific glycan composition ($[M + H]^+$, $[M + 2H]^{2+}$, $[M + 3H]^{3+}$, $[M + NH4]^+$, and $[M + 2NH4]^{2+}$). The m/z (s) and mass accuracy associated with each peak are included in Table S4.

For the isomeric profiling, *N*-glycan chromatogram peaks obtained on the same acquired raw files were used. Isomeric structures were determined based on the order in which the isomeric peaks began to elute.[47] Using FreeStyle 1.4 SP2 software, the area of glycan ions for each peak in all charge states and adduct ions was calculated to quantify the isomers. Peak areas of each glycan structure were compared to the total number of structures found in each sample, and the relative abundances of the glycans and their isomer's quantitative results were derived. These relative abundance values of the glycan isomers were used to perform an unsupervised principal component analysis (PCA) using OriginPro2022b software. Thereafter, the quantified glycans were statistically analyzed by the Mann−Whitney *U*-test and *N*-glycans including isomers with a p-value less than 0.05 were considered statistically significant.

Thereafter, the adjusted p-value (q-value) was calculated using the Benjamini−Hochberg (BH) correction. Heatmap was done with Genesis software version 1.8.1. Additionally, receiver

https://doi.org/10.1021/acsomega.4c01593
ACS Omega 2024, 9, 32628−32638

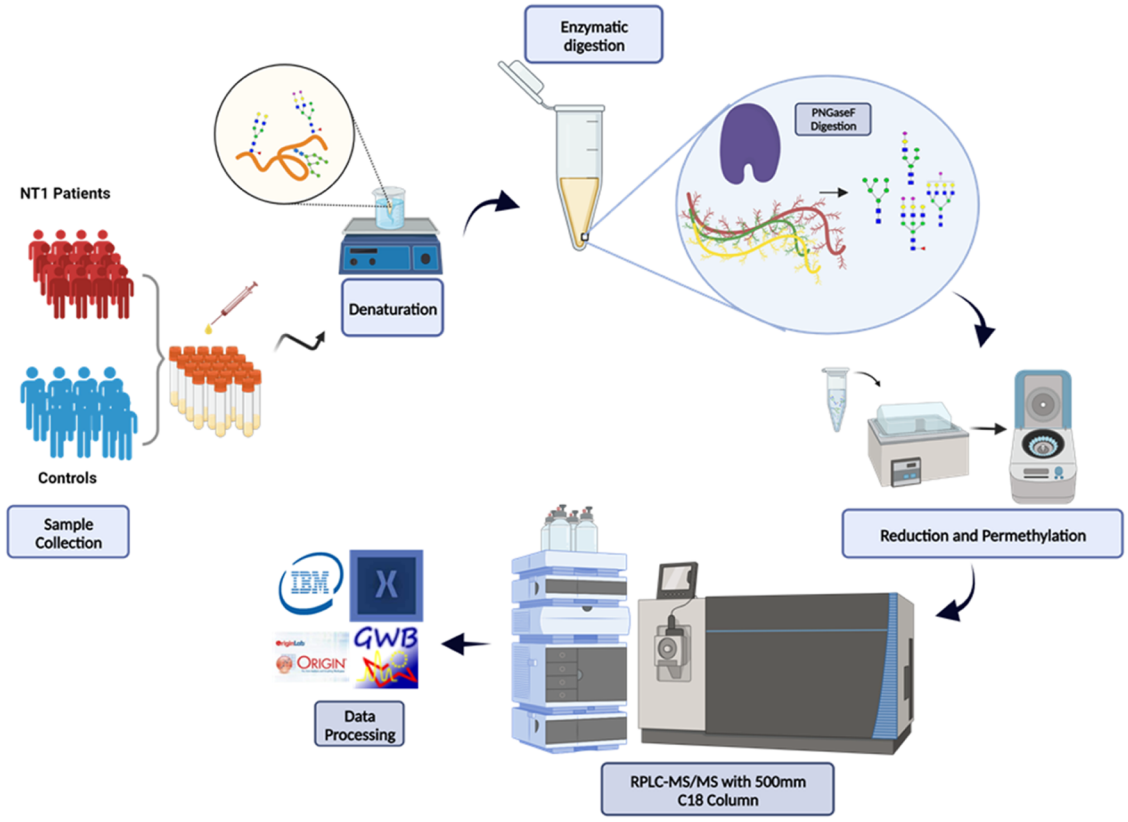

Figure 1. Workflow for the narcolepsy type 1 (NT1) glycomics experiment, outlining sample preparation and analysis. The study starts with sample collection, *N*-glycan release, solid-phase permethylation, LC-MS/MS analyses of permethylated *N*-glycans, and data processing. This image was created with BioRender.com.

operating characteristic curve (ROC) and area under curve (AUC) values were generated using SPSS version 28 (IBM) software to assess the predictive capability, selectivity, and sensitivity of each statistically significant *N*-glycan. GraphPad Prism 9.3.1 (GraphPad Software Company, La Jolla, CA) was then used to generate bar plots and boxplots.

RESULTS AND DISCUSSION

***N*-Glycan Profiling in NT1 and Healthy Serum Samples.** Profiling of *N*-glycans in NT1 and healthy control samples was completed by analyzing the redo-permethylated *N*-glycans from the serum glycoproteins on LC-MS/MS using a 500 mm C18 column. The method and sample preparation steps applied are shown in the experimental flowchart (Figure 1). The area under the EIC relative peak area integrated for each identified glycan including isomers in the control and NT1 cohorts was used for unsupervised PCA. As shown in Figure 2a, the PCA for the identified isomeric *N*-glycans shows clustering between the control cohort and the NT1 cohort at a 95% confidence level. The loading plot of PCA is shown in Figure S1. This indicates that a different *N*-glycome profile may exist for NT1. The heatmaps were conducted for the differentially expressed *N*-glycans in the healthy control cohort vs. NT1 cohorts and are shown in Figure 2b. Tables S1 and S2 show the glycan profiles in the form of relative abundance for isomeric and nonisomeric *N*-glycans in NT1 and control sample cohorts, respectively.

When the distribution of all of the identified *N*-glycan types is compared in all samples, the sialylated *N*-glycans were more abundant, followed by sialylated-fucosylated and fucosylated, while *N*-glycans with high mannose were the least abundant. Due to the higher level of sialylated *N*-glycans compared to other glycan types, the distribution of different subtypes of sialylated *N*-glycans was further explored in control and NT1 by comparing their relative abundances.

This is shown in Figure 3. Disialylated *N*-glycans were the most abundant in control and NT1 (0.33 and 0.32, respectively), followed by monosialylated (0.26 and 0.25, respectively) and trisialylated *N*-glycan (0.0075 and 0.022, respectively), and the least abundant were the tetrasialylated (0.00090 and 0.0016, respectively) *N*-glycans. Interestingly, there is a 3-fold increase in the abundance of trisialylated *N*-glycans in NT1 compared to healthy control ($p < 0.05$, based on the Mann−Whitney *U*-test followed by the BH correction).

Isomeric Quantitation of *N*-Glycans in NT1 and Healthy Serum Samples. Given the various structural complexities associated with glycans, the *N*-glycans' heterogeneity results in the existence of some glycans as isomers. While glycosylation aids the folding and stability of a protein, its roles are greatly affected by the glycan structure.[17,48,49] The identification and quantification of isomeric structures have become an essential component of glycomics investigation.[50]

Therefore, *N*-glycan isomers were equally profiled in this study using the same experimental run on LC-MS/MS with a 500 mm C18 column. The isomeric separation achieved in both NT1 and control cohorts is shown for $HexNAc_4Hex_4Fuc_1NeuAc_0$ (4410), $HexNAc_4Hex_5Fuc_1NeuAc_1$ (4511), and $HexNAc_4Hex_5Fuc_1NeuAc_0$ (4510) in Figure S2. The *N*-glycan isomers with significant variations in their glycan profiles between the NT1 and control cohorts were examined. In

https://doi.org/10.1021/acsomega.4c01593
ACS Omega 2024, 9, 32628−32638

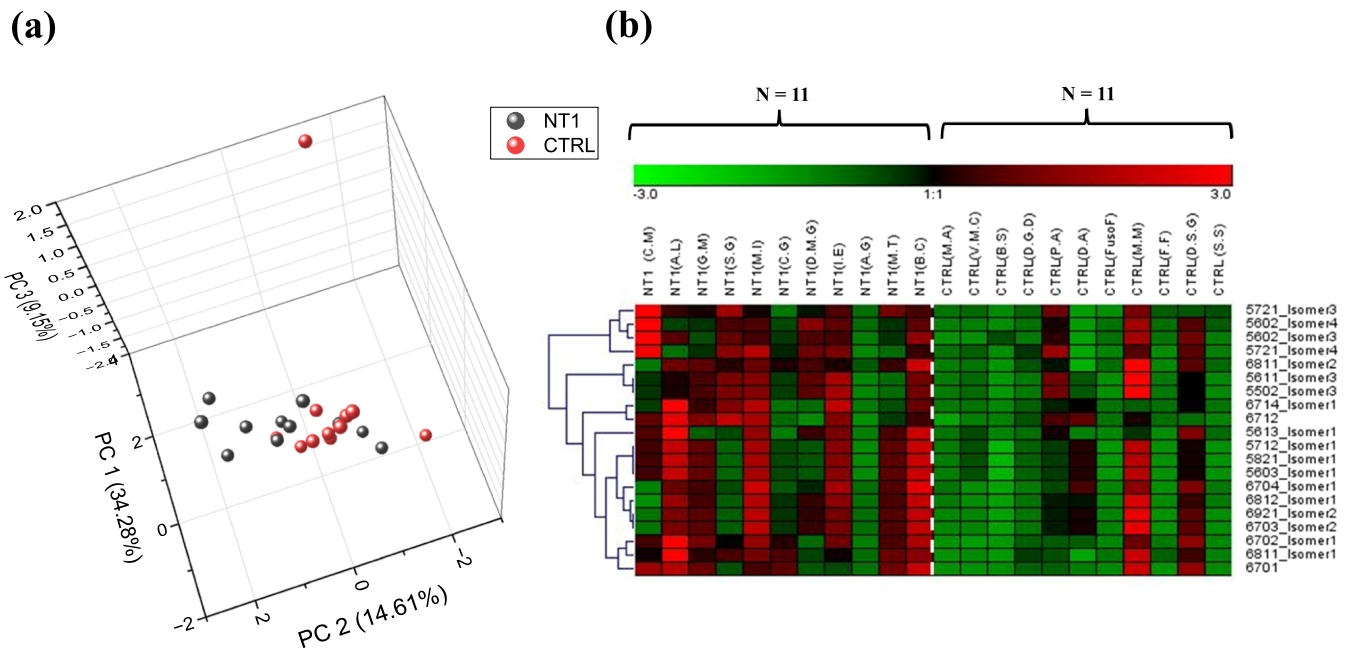

Figure 2. (a) Unsupervised principal component analysis (PCA) at a 95% confidence level for all identified *N*-glycan isomers in NT1 and control cohorts. (b) Heatmap of statistically significant *N*-glycans in NT1 vs healthy control. The red and green colors indicate upregulation and downregulation, respectively, of *N*-glycans in NT1 relative to the control. Eleven NT1 samples were compared to 11 healthy control samples.

both cohorts, a total of 18 isomeric glycan structures were found. All of the statistically significant *N*-glycan compositions were isomeric except $HexNAc_6Hex_7Fuc_0NeuAc_1$ (6701) and $HexNAc_6Hex_7Fuc_1NeuAc_2$ (6712). Among the isomeric *N*-glycan biomarker candidates, $HexNAc_5Hex_6Fuc_0NeuAc_2$ (5602), $HexNAc_5Hex_7Fuc_2NeuAc_1$ (5721), and $HexNAc_6Hex_8Fuc_1NeuAc_1$ (6811) had two isomers that were differentially expressed between the NT1 and control cohorts, while the other isomeric *N*-glycans had one differentially expressed isomer each.

Interestingly, sialylated glycans and their linkage isomers have been reported to act as receptors for the pathogenesis of influenza virus and coxackievirus.[51] In addition, aberrant level of sialylation has been determined in neurodegenerative diseases like PD and AD as the age of the patients progresses.[52,53] Table 2 includes the putative structures of *N*-glycans, the number of isomers identified, the *p*-value, the *q*-value, and the FC for each.

Statistically Significant *N*-Glycans between NT1 and Healthy Serum Samples. Descriptive statistics was applied to compare the relative abundance of *N*-glycans and their isomers in the NT1 vs control samples. Seventeen distinct *N*-glycans were statistically significant, while 15 were isomeric; the other two were nonisomeric. Again, all of the statistically significant *N*-glycans that were upregulated in the NT1 cohorts relative to the control were either sialylated or sialylayted-fucosylated. This further confirms the effect of sialylated *N*-glycans in disease development and progression, especially in brain-related diseases like Alzheimer's disease and mild cognitive impairment.[13,30,54,55] The differentially expressed glycans and isomers between the control and NT1 cohorts are shown in the form of bar graphs as well as a receiver operating characteristic curve in Figure 4a,4b, respectively. The reference line in the ROC curve is the threshold value with an AUC of 0.5. A high AUC value indicates a better selectivity, sensitivity, and predictability of each differentially expressed *N*-glycan. Interestingly, the combined ROC curve of all of the differentially expressed

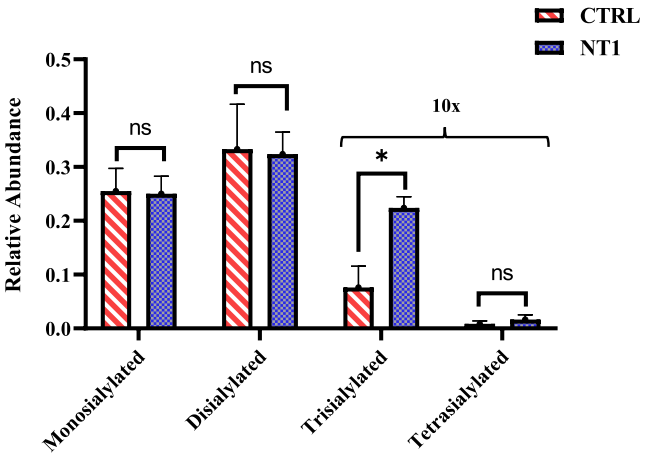

Figure 3. Distribution levels of different types of sialylated *N*-glycans in control vs NT1. The relative abundance of each type of *N*-glycan in NT1 is compared to the healthy control cohort. Only trisialylated *N*-glycans were significantly different between the two cohorts ($p < 0.05$, based on the Mann–Whitney *U*-test, followed by the BH correction). The error bar represents the standard deviation ($N = 11$).

glycans has an AUC of 1.0, which is the perfect score for ROC analysis. The *N*-glycans with the highest level of FC were $HexNAc_6Hex_7Fuc_1NeuAc_4$ (6714-1), $HexNAc_6Hex_7Fuc_0NeuAc_2$ (6702-1), and $HexNAc_6Hex_7Fuc_1NeuAc_2$ (6712) with a FC of 2.98, 2.19, and 2.07, respectively. The glycans with the most significant differences were the first isomer of $HexNAc_6Hsex_8Fuc_1NeuAc_1$ (6811-1) with a *p*-value of 0.005, $HexNAc_6Hex_7Fuc_0NeuAcs_2$ (6702-1) with a *p*-value of 0.008, and a nonisomeric *N*-glycan $HexNAc_6Hex_7Fuc_0NeuAc_1$ (6701) with a *p*-value of 0.008.

The EIC and MS/MS spectral with assigned structural fragments of four identified isomers of a differentially expressed *N*-glycan in NT1 relative to control ($HexNAc_5Hex_6Fuc_1NeuAc_3$) is shown in Figure S3. In addition, for

https://doi.org/10.1021/acsomega.4c01593
ACS Omega 2024, 9, 32628−32638

Table 2. Statistically Significant *N*-Glycans with Their *p*-Values, *q*-Values, and Fold Change (FC) in Narcolepsy Type 1 (NT1) Relative to Healthy Control Samples[a]

Putative *N*-Glycan Structures	*N*-Glycan Composition	Number of Isomers Identified	*p*-value	*q*-value	FC
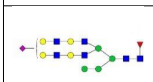	6811_Isomer 1	2	0.005	0.03	1.99
	6811_Isomer 2		0.01	0.05	1.45
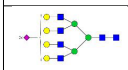	6702_Isomer 1	2	0.008	0.04	2.21
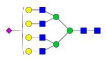	6701	none	0.008	0.04	1.77
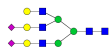	5602 Isomer 3	4	0.03	0.05	1.65
	5602_Isomer 4		0.01	0.05	1.73
	5502_Isomer 3	4	0.04	0.05	1.26
	5613_Isomer 1	4	0.01	0.05	1.95
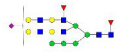	6921_Isomer 2	3	0.02	0.04	1.57
	6703_Isomer 2	3	0.02	0.04	1.91
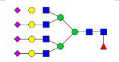	6714_Isomer 1	4	0.02	0.04	2.98
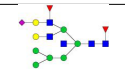	5821_Isomer 1	4	0.02	0.04	1.61
	5712_Isomer 1	4	0.02	0.04	1.62
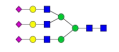	5603_Isomer 1	4	0.02	0.04	1.62
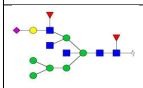	5721_Isomer 3	4	0.03	0.05	1.69
	5721_Isomer 4		0.04	0.05	1.64
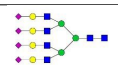	6704_Isomer 1	4	0.04	0.05	1.86
	5611_Isomer 3	4	0.04	0.05	1.26
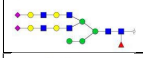	6812_Isomer 1	2	0.04	0.05	1.65
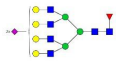	6712	none	0.04	0.05	2.07

[a]Symbols: blue box solid, *N*-acetylhexosamine; green circle solid, mannose; yellow circle solid, galactose; red triangle right-pointing solid, fucose; pink tilted square solid, *N*-acetylneuraminic acid.

better structural representation of bigger *N*-glycans including $HexNAc_6Hex_8Fuc_1NeuAc_1$, $HexNAc_5Hex_7Fuc_2NeuAc_1$, and $HexNAc_5Hex_8Fuc_2NeuAc_1$, their MS/MS spectra with assigned fragments are shown in Figure S4. These *N*-glycans can be considered potential biomarkers for NT1, which, after further validation by a larger experiment, might help distinguish between NT1 and a healthy cohort. Again, sialylated *N*-glycans, particularly the trisialylated subtype, might be playing a role in NT1 pathology or pathophysiology. In this study, $HexNAc_5Hex_6NeuAc_3$ was one of the differentially expressed trisialylated *N*-glycans that are isomeric (four isomers), and the EIC and MS/MS of each isomer, as well as the box plots of the average relative abundance of each isomer in NT1 and control cohorts, are shown in Figure 5.

The *m*/*z*, intensity, relative abundance, and charge state of $HexNAc_5Hex_6NeuAc_3$ fragments in each MS/MS spectra of the four isomers in both NT1 and control are included in Table S5.

Out of all four isomers, only the first isomer was significantly different between the two cohorts, and it was upregulated in NT1 relative to the control. The other three isomers were downregulated in NT1 without a significant difference. Previously, Dong et al. reported one of the isomers of the $HexNAc_5Hex_6NeuAc_3$ *N*-glycan as a candidate biomarker for restless leg syndrome (RLS), and thus there could be an interplay between RLS and NT1.[56] In addition, Hu et al. reported $HexNAc_5Hex_6NeuAc_3$ as the most abundant glycan and the one with the most significant increase in neuroblastoma cell lines (NLF).[57] $HexNAc_5Hex_8Fuc_3NeuAc_1$, $HexNAc_6Hex_9Fuc_2NeuAc_1$, and their EIC and MS/MS are also shown in Figure S4.

Two of the isomers of the $HexNAc_6Hex_7NeuAc_3$ *N*-glycan have been previously reported as candidate biomarkers for RLS; the first isomer (6703-1) was found to be downregulated in RLS, while the second (6703-2) was upregulated in RLS.[56] Interestingly, the same $HexNAc_6Hex_7NeuAc_3$ *N*-glycan was also identified in this study, and the second isomer was also differentially expressed.

The heavily sialylated-fucosylated *N*-glycan, $HexNAc_6Hex_7Fuc_1NeuAc_3$ (6713), has its first isomer upregulated in NT1 relative to the healthy control; although it does not meet the criteria to be statistically significant, this glycan was previously reported to exhibit higher abundances in the 231BR breast cancer cell line (a brain metastatic breast cancer cell line) relative to other breast cancer cell lines. This may suggest the role of these glycans in neurological effects that might have resulted in NT1. The isomers of the differentially expressed heavily sialylated *N*-glycans (tri and tetra sialylated) identified in this study were the most significant and exhibited the highest fold change levels.

In addition, chronic inflammation is one of the major features of autoimmune diseases like NT1, and the mechanism is often due to high levels of proinflammatory cytokines.[58] Patients of NT1 are reported to have elevated levels of proinflammatory cytokines (IL-6 and TNF-α).[59] This was also briefly revealed in proteomics study of NT1.[5] However, not only at the protein level, it has also been reported that alterations in the level of glycosylation triggers chronic inflammation.[60] Excitingly, to the best of our knowledge, this study shows the existence of a different glycome for NT1. A possible reason is the fact that the proinflammatory cytokines released in high levels control the expression of glycosyltrasnferases and the availability of the substrate for *N*-glycan biosynthesis, which in turn controls the composition of the *N*-linked oligosaccharides.[61,62]

Overall, this study of the NT1 glycome in narcoleptic patients opens the door for the scientific community to understand biomarkers indicative of autoimmune mechanisms underlying the degeneration of orexin neuropeptides, thereby elucidating the physiological basis of this disease. In general, we suggest the exploration of the sialylated and sialylated-fucosylated *N*-glycans

https://doi.org/10.1021/acsomega.4c01593
ACS Omega 2024, 9, 32628−32638

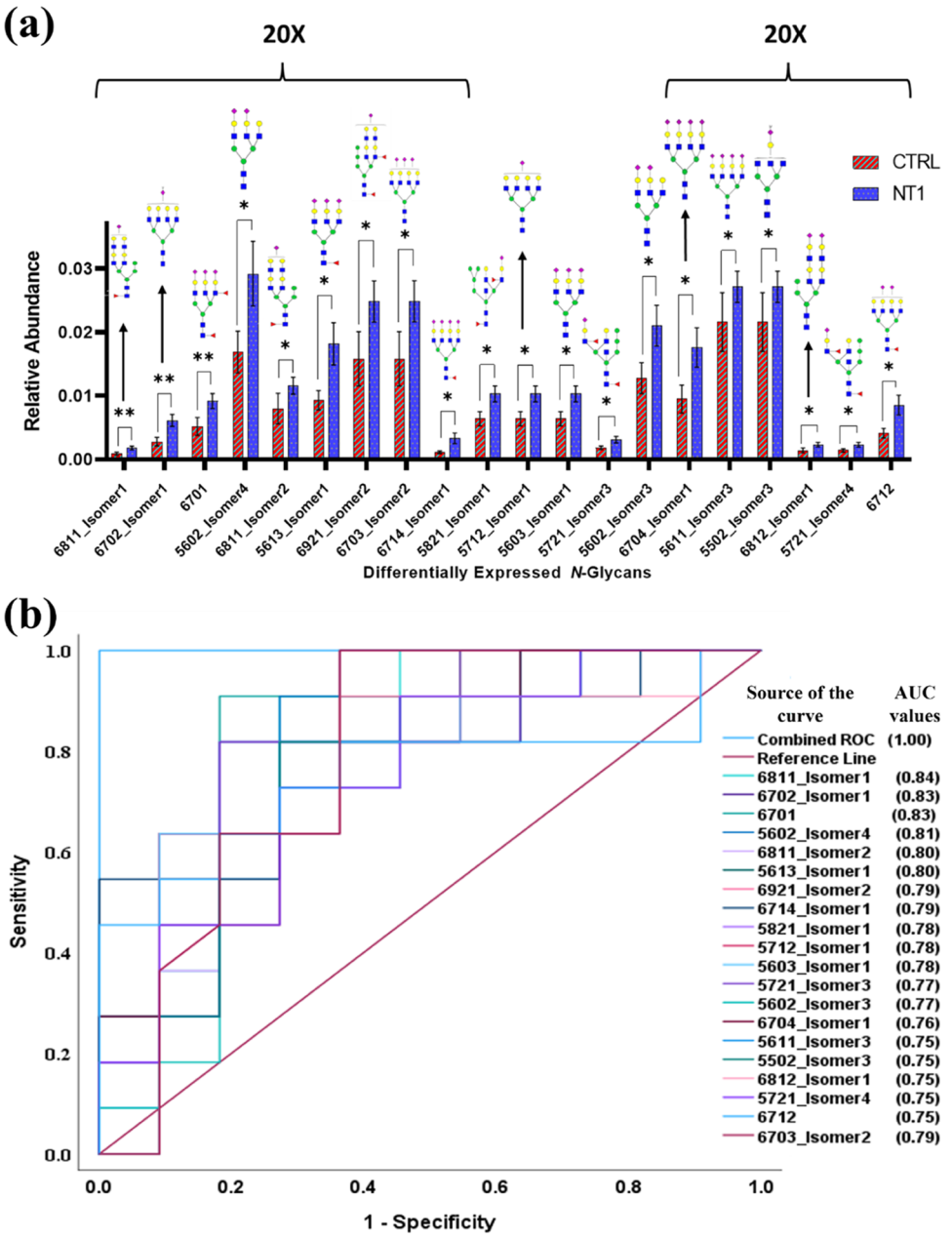

Figure 4. (a) Bar plots of statistically significant *N*-glycans in the control vs NT1 cohort, and (b) receiver operating characteristic curves and area under curves (ROC-AUC) for the statistically significant *N*-glycans and their isomers in NT1. The range of area under curve (AUC) score from the ROC analysis is 0.75−0.84, while the *p*-value is between the range of 0.01−0.04. With combined ROC analysis, the AUC was 1.0. The reference line is the threshold limit, the area under the line is 0.5, and 1.0 is the perfect value of an ROC-AUC analysis. Symbols: blue box solid, *N*-acetylhexosamine; green circle solid, mannose; yellow circle solid, galactose; red triangle right-pointing solid, fucose; pink tilted square solid, *N*-acetylneuraminic acid.

for further studies related to NT1. This could help us to better understand their roles in NT1 pathology and pathophysiology. In addition, the identification and characterization of differentially expressed *N*-glycans and their isomers in NT1 might be a good starting point to improve the understanding of the biological and biomedical mechanisms of NT1 pathogenesis.

CONCLUSIONS

In this work, we compared the serum glycan profiles of patients with NT1 and healthy controls to examine the potential for significantly different glycan expressions. Seventeen *N*-glycans and isomers, in a total of 20 candidate biomarkers, were found. The *N*-glycans that showed the greatest differences in the expression profiles were $HexNAc_6Hex_7Fuc_0NeuAc_2$ (6702) with an FC of 2.21 and $HexNAc_6Hex_7Fuc_1NeuAc_2$ (6712) with an FC of 2.07; then, isomers of $HexNAc_6Hex_7Fuc_1NeuAc_4$ (6714-1), $HexNAc_6Hex_7Fuc_0NeuAc_2$ (6702-1), and $HexNAc_6Hex_8Fuc_1NeuAc_1$ (6811-1) and with a high level of FC of 2.98, 2.21, and 1.99, respectively. Investigating the isomeric distribution in NT1 against controls allowed for in-depth comparative glycomics analysis. Interestingly, all of the differentially expressed *N*-glycans were upregulated in NT1 and were either sialylated or sialylated-fucosylated. The distribution levels of the *N*-glycans showed that trisialylated glycan types were 3-fold higher in NT1 compared to the control. We believe these

https://doi.org/10.1021/acsomega.4c01593
ACS Omega 2024, 9, 32628−32638

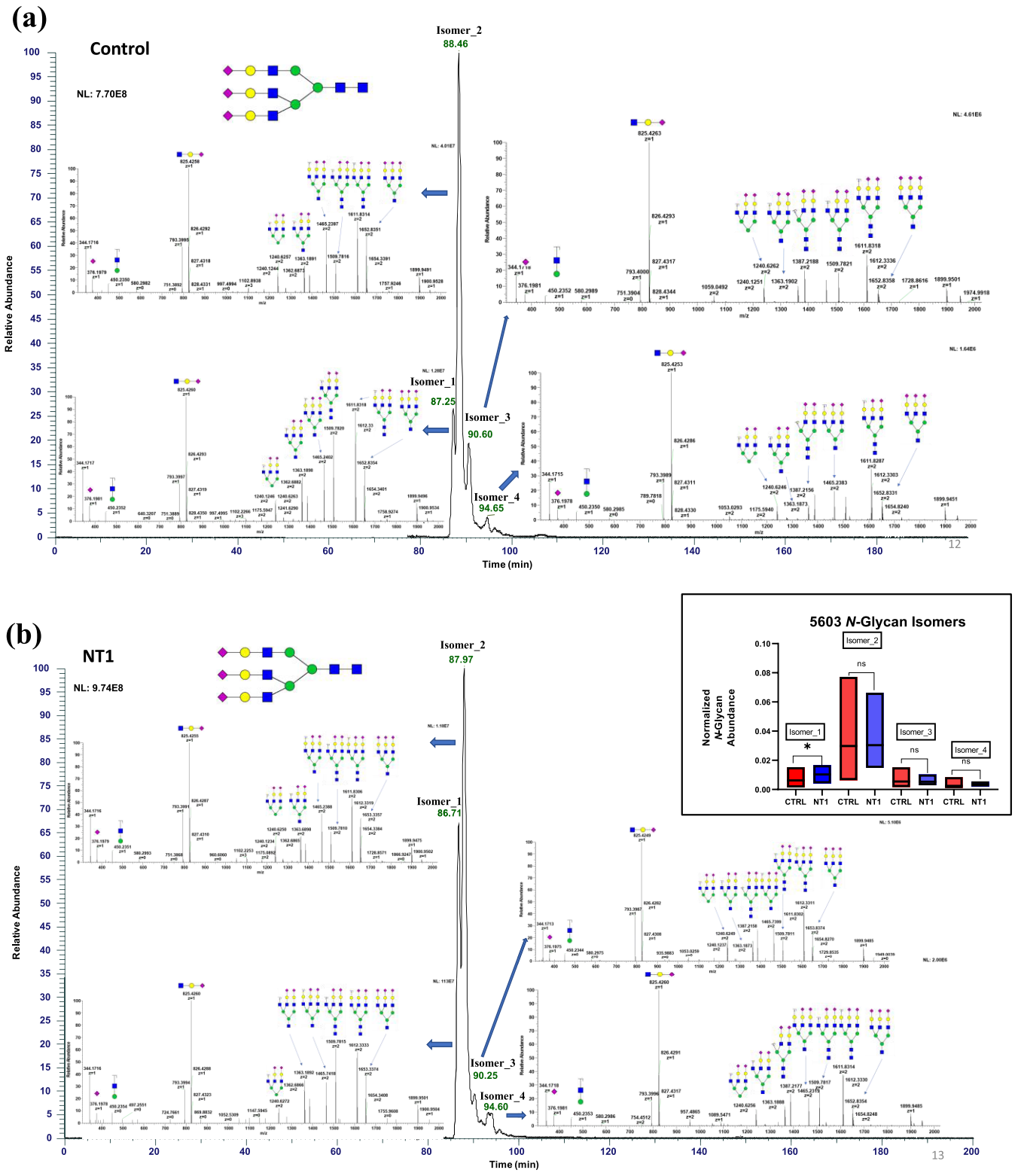

Figure 5. Representative extracted ion chromatogram (EIC) of $Hex_5Hex_6NeuAc_3$ *N*-glycan isomers separated on 500 mm C18 column (75 μm × 500 mm, 2 μm, 100 Å, Thermo Scientific, Sunnyvale, CA) in (a) control sample, and the MS/MS of the four isomers (b) NT1 sample, and the MS/MS of the four isomers. The boxplots compare the relative abundance of each of the identified isomers in control vs NT1. Symbols: blue box solid, *N*-acetylhexosamine; green circle solid, mannose; yellow circle solid, galactose; red triangle right-pointing solid, fucose; pink tilted square solid, *N*-acetylneuraminic acid.

differentially expressed glycans might be considered second-generation glycan biomarker candidates for NT1.

The evaluation of serum glycome in narcolepsy research has important clinical ramifications. First, finding glycosylation-related biomarkers in serum may help with early NT1 diagnosis and risk assessment, enabling prompt treatment and better patient outcomes. Furthermore, a better understanding of the glycome may help in the development of innovative therapeutic

https://doi.org/10.1021/acsomega.4c01593
ACS Omega 2024, 9, 32628−32638

approaches, such as immune-modulating therapies intended to stop or at least slow the loss of orexin neuropeptides. This strategy has the potential to enhance the management of narcolepsy by providing individualized treatments that address the underlying autoimmune component and enable better symptom control.

The next stage of the study will include a greater variety of samples (high number of age and gender variety), including both healthy and NT1 samples, to confirm the candidate glycan biomarkers. The role of the different linkage isomers of these identified candidate *N*-glycan biomarkers in NT1 will also be evaluated. We believe that this discovery will motivate other researchers to investigate these glycans, particularly the glycan isomers, in more detail and gain a better understanding of their biological roles in NT1 as well as other neurological diseases.

■ ASSOCIATED CONTENT

Data Availability Statement

The raw data have been submitted to GlycoPOST with the accession number GPST000306.

Supporting Information

The Supporting Information is available free of charge at https://pubs.acs.org/doi/10.1021/acsomega.4c01593.

Loading plot for the principal component analysis (PCA) of all identified *N*-glycan isomers in NT1 and control cohorts. The *N*-glycan isomers are driving the coordinates in the PCA (Figure S1). EIC showing isomeric separation of *N*-glycans and MS/MS for each isomer of (a) $HexNAc_4Hex_4Fuc_1NeuAc_0$ (4410), (b) $HexNAc_4Hex_5Fuc_1NeuAc_1$ (4511), and (c) $HexNAc_4Hex_5Fuc_1NeuAc_0$ (4510) in control and NT1. Symbols: blue box solid, *N*-acetylhexosamine; green circle solid, mannose; yellow circle solid, galactose; red triangle right-pointing solid, fucose; pink tilted square solid, *N*-acetylneuraminic acid (Figure S2). EIC and MS/MS spectra of a representative *N*-glycan ($HexNAc_5Hex_6Fuc_1NeuAc_3$ (5613)) isomers in NT1. Symbols: blue box solid, *N*-acetylhexosamine; green circle solid, mannose; yellow circle solid, galactose; red triangle right-pointing solid, fucose; pink tilted square solid, *N*-acetylneuraminic acid (Figure S3). Structural validation of bigger *N*-glycans with MS/MS. EIC and MS/MS of all identified and quantified isomers of (a) $HexNAc_6Hex_8Fuc_1NeuAc_1$ (6811), (b) $HexNAc_5Hex_7Fuc_2NeuAc_1$ (5721), (c) $HexNAc_5Hex_8Fuc_2NeuAc_1$ (5821), (d) $HexNAc_5Hex_8Fuc_3NeuAc_1$ (5831), and (e) $HexNAc_6Hex_9Fuc_2NeuAc_1$ (6921). Symbols: blue box solid, *N*-acetylhexosamine; green circle solid, mannose; yellow circle solid, galactose; red triangle right-pointing solid, fucose; pink tilted square solid, *N*-acetylneuraminic acid (Figure S4) (PDF)

Relative abundances of *N*-glycans and their isomers derived from the NT1 sample cohort acquired from the 500 mm long C18 column at 60 °C. Four-digit code refers to the monosaccharide units, *N*-acetylhexosamine, hexose, fucose, and *N*-acetylneuraminic acid, respectively. The hyphenated number indicates its isomers. **T** refers to NT1 samples (Table S1). Relative abundances of *N*-glycans and their isomers derived from the control sample cohort acquired from the 500 mm long C18 column at 60 °C. Four-digit code refers to the monosaccharide units, *N*-acetylhexosamine, hexose, fucose, and *N*-acetylneuraminic acid, respectively. The hyphenated number indicates its isomers. **C** refers to control samples (Table S2). ±SD of statistically significant *N*-glycans after applying. Glycans in the table are named according to the number of *N*-acetylhexosamine, hexose, fucose, and *N*-acetylneuraminic acid in a structure (Table S3). Respective adducts' *m*/*z* of detected *N*-glycan peaks (theoretical and observed) and their mass accuracy (ppm error) (Table S4). Tabular format of MS/MS spectra for $HexNAc_5Hex_6NeuAc_3$ (5603), $HexNAc_4Hex_4Fuc_1NeuAc_0$ (4410), $HexNAc_4Hex_5Fuc_1NeuAc_1$ (4511), $HexNAc_4Hex_5Fuc_1NeuAc_0$ (4510), $HexNAc_5Hex_6Fuc_1NeuAc_3$ (5613), $HexNAc_6Hex_8Fuc_1NeuAc_1$ (6811), $HexNAc_5Hex_7Fuc_2NeuAc_1$ (5721), $HexNAc_5Hex_8Fuc_2NeuAc_1$ (5821), $HexNAc_5Hex_8Fuc_3NeuAc_1$ (5831), and $HexNAc_6Hex_9Fuc_2NeuAc_1$ (6921) isomers, including *m*/*z*, intensity, relative abundance, and charge state of each fragment (Table S5) (XLSX)

■ AUTHOR INFORMATION

Corresponding Author

Yehia Mechref − *Chemistry and Biochemistry Department, Texas Tech University, Lubbock, Texas 79409, United States;* orcid.org/0000-0002-6661-6073; Phone: 806-834-8246; Email: yehia.mechref@ttu.edu

Authors

Akeem Sanni − *Chemistry and Biochemistry Department, Texas Tech University, Lubbock, Texas 79409, United States;* orcid.org/0000-0002-1250-7293

Md Abdul Hakim − *Chemistry and Biochemistry Department, Texas Tech University, Lubbock, Texas 79409, United States*

Mona Goli − *Chemistry and Biochemistry Department, Texas Tech University, Lubbock, Texas 79409, United States*

Moyinoluwa Adeniyi − *Chemistry and Biochemistry Department, Texas Tech University, Lubbock, Texas 79409, United States*

Farid Talih − *Department of Psychiatry, Faculty of Medicine, American University of Beirut, Beirut 1107 2020, Lebanon*

Bartolo Lanuzza − *Sleep Research Centre, Department of Neurology IC, Oasi Research Institute-IRCCS, Troina 94018, Italy*

Firas Kobeissy − *Department of Biochemistry and Molecular Genetics, Faculty of Medicine, American University of Beirut, Beirut 1107 2020, Lebanon; Department of Neurobiology, Center for Neurotrauma, Multiomics and Biomarkers (CNMB), Neuroscience Institute, Morehouse School of Medicine (MSM), Atlanta, Georgia 30310-1458, United States*

Giuseppe Plazzi − *IRCCS, Istituto delle Scienze Neurologiche di Bologna, Bologna 40138, Italy; Department of Biomedical, Metabolic and Neural Sciences, University of Modena and Reggio Emilia, Modena 41121, Italy*

Monica Moresco − *IRCCS, Istituto delle Scienze Neurologiche di Bologna, Bologna 40138, Italy*

Stefania Mondello − *Department of Biomedical and Dental Sciences and Morphofunctional Imaging, University of Messina, Messina 98122, Italy*

Raffaele Ferri − *Sleep Research Centre, Department of Neurology IC, Oasi Research Institute-IRCCS, Troina 94018, Italy*

https://doi.org/10.1021/acsomega.4c01593
ACS Omega 2024, 9, 32628−32638

Complete contact information is available at:
https://pubs.acs.org/10.1021/acsomega.4c01593

Author Contributions

◆A.S. and M.A.H. contributed equally to this work. The manuscript was written through contributions of all authors. Y.M., R.F., G.P., and S.M. conceptualized experiments and provided the funding. Y.M., R.F., and F.K. supervised the project. A.S. developed the method, performed formal analysis, and validated and wrote the original draft of the manuscript. A.S. and M.A.H. did the sample preparation and curated the data. M.G., M.A., G.P., F.T., B.L., M.M., and Y.M. reviewed and edited the manuscript. All authors have given approval to the final version of the manuscript.

Funding

This work was supported by grants from the National Institutes of Health: 1R01GM112490-09 (Y.M.), 1R01GM130091-04 (Y.M.), and the Italian Ministry of Health Ricerca Corrente (RC), Grant/Award Number 27773803 (R.F.). This work was also supported by the Robert A. Welch Foundation under grant number D-0005 (Y.M.) and The CH Foundation.

Notes

The authors declare no competing financial interest.

■ ACKNOWLEDGMENTS

The authors thank members of Mechref Omics Lab and Prof. Ferri's laboratory for helpful discussions.

■ ABBREVIATIONS

NT1, narcolepsy type 1; CID, collision-induced dissociation; HCD, high-energy collision dissociation; EThcD, electron-transfer/higher-energy collision dissociation; NMR, nuclear magnetic resonance; REM, rapid eye movement; HLA, human leukocyte antigen; PCA, principal component analysis; EIC, extracted ion chromatogram

■ REFERENCES

(1) Chavda, V.; Chaurasia, B.; Umana, G. E.; Tomasi, S. O.; Lu, B.; Montemurro, N. Narcolepsy-A Neuropathological Obscure Sleep Disorder: A Narrative Review of Current Literature. *Brain Sci.* **2022**, *12* (11), 1473 DOI: 10.3390/brainsci12111473.

(2) Kornum, B. R.; Knudsen, S.; Ollila, H. M.; Pizza, F.; Jennum, P. J.; Dauvilliers, Y.; Overeem, S. Narcolepsy. *Nat. Rev. Dis. Primers* **2017**, *3*, No. 16100, DOI: 10.1038/nrdp.2016.100.

(3) Ollila, H. M. Narcolepsy type 1: what have we learned from genetics? *Sleep* **2020**, *43* (11), No. zsaa099, DOI: 10.1093/sleep/zsaa099.

(4) Wang, Y.; Sun, Q.; Tang, Q.; Zhang, Y.; Tang, M.; Wang, D.; Wang, Z. Progress of autonomic disturbances in narcolepsy type 1. *Front. Neurol* **2023**, *14*, No. 1107632.

(5) Sanni, A.; Goli, M.; Zhao, J.; Wang, J.; Barsa, C.; El Hayek, S.; Talih, F.; Lanuzza, B.; Kobeissy, F.; Plazzi, G.; et al. LC-MS/MS-Based Proteomics Approach for the Identification of Candidate Serum Biomarkers in Patients with Narcolepsy Type 1. *Biomolecules* **2023**, *13* (3), 420.

(6) Mikolajczyk, K.; Kaczmarek, R.; Czerwinski, M. How glycosylation affects glycosylation: the role of N-glycans in glycosyltransferase activity. *Glycobiology* **2020**, *30* (12), 941−969.

(7) Eichler, J. Protein glycosylation. *Curr. Biol.* **2019**, *29* (7), R229−R231, DOI: 10.1016/j.cub.2019.01.003.

(8) Kobeissy, F.; Kobaisi, A.; Peng, W.; Barsa, C.; Goli, M.; Sibahi, A.; El Hayek, S.; Abdelhady, S.; Ali Haidar, M.; Sabra, M.; et al. Glycomic and Glycoproteomic Techniques in Neurodegenerative Disorders and Neurotrauma: Towards Personalized Markers. *Cells* **2022**, *11* (3), 581 DOI: 10.3390/cells11030581.

(9) Viswanathan, K.; Chandrasekaran, A.; Srinivasan, A.; Raman, R.; Sasisekharan, V.; Sasisekharan, R. Glycans as receptors for influenza pathogenesis. *Glycoconjugate J.* **2010**, *27* (6), 561−570.

(10) Gutierrez Reyes, C. D.; Jiang, P.; Donohoo, K.; Atashi, M.; Mechref, Y. S. Glycomics and glycoproteomics: Approaches to address isomeric separation of glycans and glycopeptides. *J. Sep. Sci.* **2021**, *44* (1), 403−425.

(11) Adamczyk, B.; Tharmalingam, T.; Rudd, P. M. Glycans as cancer biomarkers. *Biochim. Biophys. Acta* **2012**, *1820* (9), 1347−1353.

(12) Leiserowitz, G. S.; Lebrilla, C.; Miyamoto, S.; An, H. J.; Duong, H.; Kirmiz, C.; Li, B.; Liu, H.; Lam, K. S. Glycomics analysis of serum: a potential new biomarker for ovarian cancer? *Int. J. Gynecol. Cancer* **2008**, *18* (3), 470−475.

(13) Palmigiano, A.; Barone, R.; Sturiale, L.; Sanfilippo, C.; Bua, R. O.; Romeo, D. A.; Messina, A.; Capuana, M. L.; Maci, T.; Le Pira, F.; et al. CSF N-glycoproteomics for early diagnosis in Alzheimer's disease. *J. Proteomics* **2016**, *131*, 29−37.

(14) Russell, A. C.; Šimurina, M.; Garcia, M. T.; Novokmet, M.; Wang, Y.; Rudan, I.; Campbell, H.; Lauc, G.; Thomas, M. G.; Wang, W. The N-glycosylation of immunoglobulin G as a novel biomarker of Parkinson's disease. *Glycobiology* **2017**, *27* (5), 501−510.

(15) Dube, D. H.; Bertozzi, C. R. Glycans in cancer and inflammation−potential for therapeutics and diagnostics. *Nat. Rev. Drug Discovery* **2005**, *4* (6), 477−488.

(16) Ben Faleh, A.; Warnke, S.; Bansal, P.; Pellegrinelli, R. P.; Dyukova, I.; Rizzo, T. R. Identification of Mobility-Resolved N-Glycan Isomers. *Anal. Chem.* **2022**, *94* (28), 10101−10108.

(17) Peng, W.; Goli, M.; Mirzaei, P.; Mechref, Y. Revealing the Biological Attributes of N-Glycan Isomers in Breast Cancer Brain Metastasis Using Porous Graphitic Carbon (PGC) Liquid Chromatography-Tandem Mass Spectrometry (LC-MS/MS). *J. Proteome Res.* **2019**, *18* (10), 3731−3740.

(18) Veillon, L.; Huang, Y.; Peng, W.; Dong, X.; Cho, B. G.; Mechref, Y. Characterization of isomeric glycan structures by LC-MS/MS. *Electrophoresis* **2017**, *38* (17), 2100−2114.

(19) Wang, J.; Dong, X.; Yu, A.; Huang, Y.; Peng, W.; Mechref, Y. Isomeric separation of permethylated glycans by extra-long reversed-phase liquid chromatography (RPLC)-MS/MS. *Analyst* **2022**, *147* (10), 2048−2059.

(20) Lundborg, M.; Fontana, C.; Widmalm, G. Automatic structure determination of regular polysaccharides based solely on NMR spectroscopy. *Biomacromolecules* **2011**, *12* (11), 3851−3855.

(21) Zhang, R.; Peng, W.; Huang, Y.; Gautam, S.; Wang, J.; Mechref, Y.; Tang, H. A Reciprocal Best-hit Approach to Characterize Isomeric N-Glycans Using Tandem Mass Spectrometry. *Anal. Chem.* **2022**, *94* (28), 10003−10010.

(22) Daramola, O.; Gutierrez-Reyes, C. D.; Wang, J.; Nwaiwu, J.; Onigbinde, S.; Fowowe, M.; Dominguez, M.; Mechref, Y. Isomeric separation of native N-glycans using nano zwitterionic- hydrophilic interaction liquid chromatography column. *J. Chromatogr. A* **2023**, *1705*, No. 464198.

(23) Zhou, S.; Veillon, L.; Dong, X.; Huang, Y.; Mechref, Y. Direct comparison of derivatization strategies for LC-MS/MS analysis of N-glycans. *Analyst* **2017**, *142* (23), 4446−4455.

(24) Kang, P.; Mechref, Y.; Novotny, M. V. High-throughput solid-phase permethylation of glycans prior to mass spectrometry. *Rapid Commun. Mass Spectrom.* **2008**, *22* (5), 721−734.

(25) Zhou, S.; Wooding, K. M.; Mechref, Y. Analysis of Permethylated Glycan by Liquid Chromatography (LC) and Mass Spectrometry (MS). *Methods Mol. Biol.* **2017**, *1503*, 83−96.

(26) Zaia, J. Mass spectrometry of oligosaccharides. *Mass Spectrom. Rev.* **2004**, *23* (3), 161−227.

(27) Melmer, M.; Stangler, T.; Schiefermeier, M.; Brunner, W.; Toll, H.; Rupprechter, A.; Lindner, W.; Premstaller, A. HILIC analysis of fluorescence-labeled N-glycans from recombinant biopharmaceuticals. *Anal. Bioanal. Chem.* **2010**, *398* (2), 905−914.

(28) Mancera-Arteu, M.; Giménez, E.; Barbosa, J.; Sanz-Nebot, V. Identification and characterization of isomeric N-glycans of human alfa-acid-glycoprotein by stable isotope labelling and ZIC-HILIC-MS in

combination with exoglycosidase digestion. *Anal. Chim. Acta* **2016**, *940*, 92−103.
(29) Vreeker, G. C. M.; Wuhrer, M. Reversed-phase separation methods for glycan analysis. *Anal. Bioanal. Chem.* **2017**, *409* (2), 359−378.
(30) Reyes, C. D. G.; Hakim, M. A.; Atashi, M.; Goli, M.; Gautam, S.; Wang, J.; Bennett, A. I.; Zhu, J.; Lubman, D. M.; Mechref, Y. LC-MS/MS Isomeric Profiling of N-Glycans Derived from Low-Abundant Serum Glycoproteins in Mild Cognitive Impairment Patients. *Biomolecules* **2022**, *12* (11), 1657 DOI: 10.3390/biom12111657.
(31) Gillmeister, M. P.; Tomiya, N.; Jacobia, S. J.; Lee, Y. C.; Gorfien, S. F.; Betenbaugh, M. J. An HPLC-MALDI MS method for N-glycan analyses using smaller size samples: application to monitor glycan modulation by medium conditions. *Glycoconjugate J.* **2009**, *26* (9), 1135−1149.
(32) Zhou, S.; Hu, Y.; Mechref, Y. High-temperature LC-MS/MS of permethylated glycans derived from glycoproteins. *Electrophoresis* **2016**, *37* (11), 1506−1513.
(33) Nilsson, J. Liquid chromatography-tandem mass spectrometry-based fragmentation analysis of glycopeptides. *Glycoconjugate J.* **2016**, *33* (3), 261−272.
(34) Yu, Q.; Wang, B.; Chen, Z.; Urabe, G.; Glover, M. S.; Shi, X.; Guo, L. W.; Kent, K. C.; Li, L. Electron-Transfer/Higher-Energy Collision Dissociation (EThcD)-Enabled Intact Glycopeptide/Glycoproteome Characterization. *J. Am. Soc. Mass Spectrom.* **2017**, *28* (9), 1751−1764.
(35) Neagu, A. N.; Jayathirtha, M.; Baxter, E.; Donnelly, M.; Petre, B. A.; Darie, C. C. Applications of Tandem Mass Spectrometry (MS/MS) in Protein Analysis for Biomedical Research. *Molecules* **2022**, *27* (8), 2411 DOI: 10.3390/molecules27082411.
(36) Peng, W.; Gutierrez Reyes, C. D.; Gautam, S.; Yu, A.; Cho, B. G.; Goli, M.; Donohoo, K.; Mondello, S.; Kobeissy, F.; Mechref, Y. MS-based glycomics and glycoproteomics methods enabling isomeric characterization. *Mass Spectrom. Rev.* **2023**, *42* (2), 577−616.
(37) Sanni, A.; Goli, M.; Zhao, J.; Wang, J.; Barsa, C.; El Hayek, S.; Talih, F.; Lanuzza, B.; Kobeissy, F.; Plazzi, G.; et al. LC-MS/MS-Based Proteomics Approach for the Identification of Candidate Serum Biomarkers in Patients with Narcolepsy Type 1. *Biomolecules* **2023**, *13* (3), 420 DOI: 10.3390/biom13030420.
(38) Thüring, K.; Schmid, K.; Keller, P.; Helm, M. LC-MS Analysis of Methylated RNA. *Methods Mol. Biol.* **2017**, *1562*, 3−18.
(39) Li, Q.; Sun, M.; Yu, M.; Fu, Q.; Jiang, H.; Yu, G.; Li, G. Gangliosides profiling in serum of breast cancer patient: GM3 as a potential diagnostic biomarker. *Glycoconjugate J.* **2019**, *36* (5), 419−428.
(40) Crutchfield, C. A.; Thomas, S. N.; Sokoll, L. J.; Chan, D. W. Advances in mass spectrometry-based clinical biomarker discovery. *Clin. Proteomics* **2016**, *13*, 1.
(41) Ma, X. Recent Advances in Mass Spectrometry-Based Structural Elucidation Techniques. *Molecules* **2022**, *27* (19), 6466 DOI: 10.3390/molecules27196466.
(42) Cartwright, R. D. Alcohol and NREM parasomnias: evidence versus opinions in the international classification of sleep disorders, 3rd edition. *J. Clin. Sleep Med.* **2014**, *10* (9), 1039−1040, DOI: 10.5664/jcsm.4050.
(43) Rose, N. R.; Bona, C. Defining criteria for autoimmune diseases (Witebsky's postulates revisited). *Immunol. Today* **1993**, *14* (9), 426−430.
(44) Giannoccaro, M. P.; Liguori, R.; Plazzi, G.; Pizza, F. Reviewing the Clinical Implications of Treating Narcolepsy as an Autoimmune Disorder. *Nat. Sci. Sleep* **2021**, *13*, 557−577, DOI: 10.2147/NSS.S275931.
(45) Liblau, R. S.; Latorre, D.; Kornum, B. R.; Dauvilliers, Y.; Mignot, E. J. The immunopathogenesis of narcolepsy type 1. *Nat. Rev. Immunol.* **2024**, *24* (1), 33−48.
(46) Kang, P.; Mechref, Y.; Klouckova, I.; Novotny, M. V. Solid-phase permethylation of glycans for mass spectrometric analysis. *Rapid Commun. Mass Spectrom.* **2005**, *19* (23), 3421−3428.
(47) Zhou, S.; Dong, X.; Veillon, L.; Huang, Y.; Mechref, Y. LC-MS/MS analysis of permethylated N-glycans facilitating isomeric characterization. *Anal. Bioanal. Chem.* **2017**, *409* (2), 453−466.
(48) Xu, C.; Ng, D. T. Glycosylation-directed quality control of protein folding. *Nat. Rev. Mol. Cell Biol.* **2015**, *16* (12), 742−752.
(49) Gavrilov, Y.; Shental-Bechor, D.; Greenblatt, H. M.; Levy, Y. Glycosylation May Reduce Protein Thermodynamic Stability by Inducing a Conformational Distortion. *J. Phys. Chem. Lett.* **2015**, *6* (18), 3572−3577.
(50) Varki, A. Biological roles of glycans. *Glycobiology* **2017**, *27* (1), 3−49.
(51) Nilsson, E. C.; Jamshidi, F.; Johansson, S. M.; Oberste, M. S.; Arnberg, N. Sialic acid is a cellular receptor for coxsackievirus A24 variant, an emerging virus with pandemic potential. *J. Virol.* **2008**, *82* (6), 3061−3068.
(52) Váradi, C.; Nehéz, K.; Hornyák, O.; Viskolcz, B.; Bones, J. Serum N-Glycosylation in Parkinson's Disease: A Novel Approach for Potential Alterations. *Molecules* **2019**, *24* (12), 2220 DOI: 10.3390/molecules24122220.
(53) Kanninen, K.; Goldsteins, G.; Auriola, S.; Alafuzoff, I.; Koistinaho, J. Glycosylation changes in Alzheimer's disease as revealed by a proteomic approach. *Neurosci. Lett.* **2004**, *367* (2), 235−240.
(54) Liu, F.; Simpson, A. B.; D'Costa, E.; Bunn, F. S.; van Leeuwen, S. S. Sialic acid, the secret gift for the brain. *Crit. Rev. Food Sci. Nutr.* **2023**, *63* (29), 9875−9894, DOI: 10.1080/10408398.2022.2072270.
(55) Cuello, H. A.; Ferreira, G. M.; Gulino, C. A.; Toledo, A. G.; Segatori, V. I.; Gabri, M. R. Terminally sialylated and fucosylated complex N-glycans are involved in the malignant behavior of high-grade glioma. *Oncotarget* **2020**, *11* (52), 4822−4835.
(56) Dong, X.; Mondello, S.; Kobeissy, F.; Ferri, R.; Mechref, Y. Serum Glycomics Profiling of Patients with Primary Restless Legs Syndrome Using LC-MS/MS. *J. Proteome Res.* **2020**, *19* (8), 2933−2941.
(57) Hu, Y.; Mayampurath, A.; Khan, S.; Cohen, J. K.; Mechref, Y.; Volchenboum, S. L. N-linked glycan profiling in neuroblastoma cell lines. *J. Proteome Res.* **2015**, *14* (5), 2074−2081.
(58) Wright, T. M.; Wright, T. M. Cytokines in acute and chronic inflammation. *Front. Biosci.* **1997**, *2*, d12−d26.
(59) Mohammadi, S.; Mayeli, M.; Saghazadeh, A.; Rezaei, N. Cytokines in narcolepsy: A systematic review and meta-analysis. *Cytokine* **2020**, *131*, No. 155103.
(60) Groux-Degroote, S.; Cavdarli, S.; Uchimura, K.; Allain, F.; Delannoy, P. Glycosylation changes in inflammatory diseases. *Adv. Protein Chem. Struct. Biol.* **2020**, *119*, 111−156.
(61) Dewald, J. H.; Colomb, F.; Bobowski-Gerard, M.; Groux-Degroote, S.; Delannoy, P. Role of Cytokine-Induced Glycosylation Changes in Regulating Cell Interactions and Cell Signaling in Inflammatory Diseases and Cancer. *Cells* **2016**, *5* (4), 43 DOI: 10.3390/cells5040043.
(62) Radovani, B.; Gudelj, I. N-Glycosylation and Inflammation; the Not-So-Sweet Relation. *Front. Immunol.* **2022**, *13*, No. 893365.

https://doi.org/10.1021/acsomega.4c01593
ACS Omega 2024, 9, 32628−32638